CHEMICAL ENGINEERING TRANSACTIONS
VOL. 86, 2021
A publication of AIDIC
The Italian Association of Chemical Engineering
Online at www.cetjournal.it
Guest Editors: Sauro Pierucci, Jiří Jaromír Klemeš

ISBN 978-88-95608-84-6; **ISSN** 2283-9216
DOI: 10.3303/CET2186116

Transport of an Eco-friendly L70-C Bio-based Sucrose Ester Surfactant: Implication for Soil Remediation Purposes

Benjamin Dussaussoy, Audrey Drelich, Edvina Lamy*

Alliance Sorbonne Université, Université de Technologie de Compiègne, UTC/ESCOM, EA 4297 TIMR, Centre de recherche Royallieu - CS 60 319 - 60 203 Compiègne cedex, France.
edvina.lamy@utc.fr

Due to their biodegradability and low toxicity bio-based surfactants are very promising for use in remediation technologies, particularly for hydrocarbon contaminated soils. To enhance the application of surfactant-based technologies for remediation of organic contaminated sites, it is important to have a better understanding of the surfactant transport and retention mechanisms involved in this process, as they will impact the remediation efficiency. In this work, transport and retention mechanisms of an industrial bio-based nonionic sucrose ester surfactant were investigated through batch and column experiments, carried out on sandy porous media under saturated steady state flow conditions. Column transport experiments were conducted at surfactant concentrations ranged from 1 to 10 CMC (critical micellar concentration), for two distinct Darcy flow rates (0.35 and 0.70 $cm.min^{-1}$). Surfactant transport and retention parameters were estimated by fitting a convection-diffusion transport model (implemented on HYDRUS-1D code) to the observed transport breakthrough curves, in order to provide an adequate description and understanding of the mechanisms involved in the transport and adsorption of these compounds through porous media. The results obtained from column experiments performed under high flow rate combined with high surfactant concentration provided the best conditions for high surfactant recovery in the effluent and low surfactant adsorption rate onto the sand. Numerical HYDRUS-1D simulations permitted to quantify surfactant transport behavior and provided attachment coefficients several order of magnitude greater than detachment coefficients, indicating that surfactant retention was an irreversible process.

1. Introduction

Due to their amphiphilic structure, surfactants molecules are able to reduce interfacial tension and to increase the apparent solubility of hydrophobic compounds such as hydrocarbons in aqueous solution, thanks to micellar structure formation (Almeida et al., 2018). For this reason, they are used in surfactant-enhanced soil remediation technology for hydrocarbon contaminated soils (Mulligan, 2017). Among the cationic, anionic, nonionic and zwitterionic surfactant, nonionic surfactants have lower toxicity and best solubilization capacity (Mao et al., 2015). Most of common surfactant molecules, such as Triton X100 or Brij 35, originate from fossil resources and they often present not suitable results for toxicity, biodegradability and biocompatibility (Lau et al., 2014). However, with the recent improvement of bioprocesses, new industrial surfactants with higher biodegradability and lower toxicity are available (Almeida et al., 2019). These recent advances in bioprocess had managed to improve bio-based surfactant cost efficiency, which is a limiting factor for their use in soil remediation. New industrial bio-based surfactants currently available for remediation purposes include sucrose esters, alkylpolyglucosides and the biological surfactants such as rhamnolipids and lipopeptides. Sucrose esters, widely used in cosmetic and food industries, could be a good alternative in soil remediation and some recent works using sucrose esters have highlighted enhancement of biodegradation of hydrophobic compounds (Yin et al., 2016).
The surfactant efficiency in remediation processes is strongly dependent to the surfactant concentration and structure, the temperature and the presence of other components in the solution such as salts (Rosen and Kunjappu, 2012). The best results for soil remediation washing process powered by surfactant are obtained when the surfactant concentration is higher than the critical micellar concentration (CMC) (Mao et al., 2015).

Paper Received: 11 October 2020; Revised: 19 March 2021; Accepted: 6 April 2021
Please cite this article as: Dussaussoy B., Drelich A., Lamy E., 2021, Transport of an Eco-friendly L70-c Bio-based Sucrose Ester Surfactant: Implication for Soil Remediation Purposes, Chemical Engineering Transactions, 86, 691-696 DOI:10.3303/CET2186116

Above this concentration, surfactant monomers form aggregates called micelles. The ability of a surfactant to enhance hydrophobic pollutant desorption is generally evaluated in batch or laboratory column systems (Cecotti et al., 2018). Some surfactants can have a negative action during their transport in the porous medium, causing clogging of the pores and thus reducing soil permeability. The heterogeneity of the soil affects the hydrodynamics of the porous medium, which in turn will impact the transport mechanisms. Indeed, soil remediation by surfactants is less effective in the case of heterogeneous soils with macroporosities. Therefore, a preferential transport of surfactants occurs within the larger pores of the medium, reducing the pollutant/ surfactant contact zones and thus, the treatment efficiency. The dynamic mass transport and the interaction of surfactants with soil particles are key factors to propose appropriate solutions for soil remediation, because they may significantly impact the pollutant mobilization and thus the remediation efficiency.

Batch and column transport experiments using a bio-based surfactant (Sisterna L70-C) were performed in this work to investigate transport and retention of this molecule and investigate its potential use for soil remediation. This new nonionic sucrose ester surfactant was selected considering economic and environmental stress. Surfactant transport in sandy column experiments was compared to that of a non-reactive molecule tracer (potassium-bromide). Transport and retention experiments at various conditions (flowrate and concentration) permitted to point out some operational conditions for the optimal use in soil remediation. Numerical simulations with Hydrus-1D code were also performed to characterize water flow, to estimate sucrose ester surfactant transport and deposition parameters.

2. Materials and methods

2.1 Surfactant characterization and batch experiments

The commercial L70-C bio-based nonionic sucrose ester surfactant purchased from Sisterna used in this study was composed of α-D-Glucopyranoside, β-D-fructofuranosyl, dodecanoate, mixed with ethanol and water. It had a pH 7 and a purity equal to 37.9 %. High-purity water was used to prepare aqueous surfactant solutions from 2 10^{-5} mol.L^{-1} to 1 10^{-2} mol.L^{-1}, with a magnetic stirrer. Surface tension measurements were carried out using a K100 tensiometer (KRÜSS) with a Wilhelmy plate to determine CMC, surface tension at CMC and surface excess (Γ). The CMC was determined when the surface tension reaches a minimum and remains constant. The surface excess Γ [mol.m^{-2}] of the surfactant at the CMC was estimated by the surface tension Gibbs equation (Rosen and Kunjappu, 2012). Surfactant zeta potential was 0.69 $\pm$ 1.13 mV. Surfactant concentration in aqueous media was estimated by DNS colorimetric dosing (Mercado-Pacheco et al., 2020). Characteristics of Sisterna L70C were compared to the existing literature data obtained for two nonionic conventional Triton X100 and Brij 35 surfactants, widely used in soil remediation (Bhairi et al., 2017). A CMC $\approx$ 10^{-4} mol.L^{-1} was found for Sisterna L70-C, similar to that of Brij 35 (10^{-4} mol.L^{-1}) but lower than that of Triton X100 (23*10^{-4} mol.L^{-1}). As it is necessary to work with concentration above the CMC (Mao et al., 2015), Sisterna L70-C low CMC will lead to a decrease of surfactant consumption (Paria, 2008). The surface tension reached at the CMC was about 29 mN.m^{-1}, similarly to Triton X100, but lower than that of Brij 35. Low surface tension may enhance pollutant mobilization and solubilization (Salager et al., 2017). The surface excess reached, $\Gamma \approx$ 1,16 10^{-6} mol.m^{-2} for Sisterna L70-C compared to 3.46 10^{-6} for Triton X100 and 1.64 10^{-6} for Brij 35.

Surfactant's adsorption experiments were carried out in a natural coarse sand sampled at Compiègne (France), exhibiting a particle size distribution of 0.36-1.90 mm with a median grain size (d_{50}) of 1.01mm, a specific surface of 2.80 $\pm$ 0.08 $m^2.g^{-1}$ and a zeta potential of -23.2 $\pm$ 2.2 mV. To determine time to pseudo equilibrium (Gabet, 2004), 3.00 g of sand was mixed with 10.0 mL of surfactant at 1 CMC (critical micellar concentration) in a brown glass bottle. The surfactant adsorption rate and adsorption velocity were then estimated.

2.2 Column transport experiments

A vertically oriented column of 17 cm in length and 3.3 cm in diameter was filled with the same sand as that used for batch experiments. It was then saturated from the bottom to the top by a 10^{-4} mol.L^{-1} NaCl background electrolyte solution (Figure 1), using a peristaltic pump Ismatec ISM828B, IDEX corporation. The total porosity of the sand, ranging from 43 to 47%, was calculated from its bulk density. The later was estimated after packing the columns. The mean total pore volume (V_0), obtained by weighting each column before and after water saturation reached 62.8 $\pm$ 1.9 cm^3.

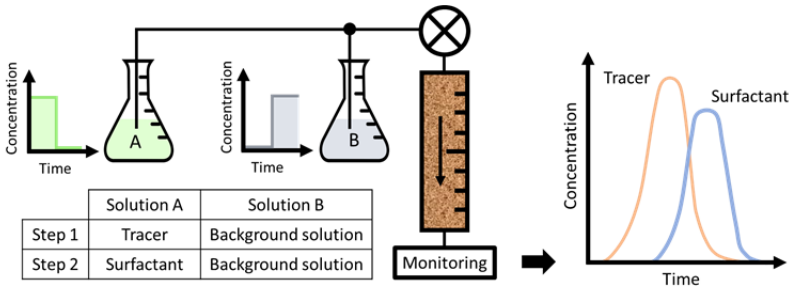

	Solution A	Solution B
Step 1	Tracer	Background solution
Step 2	Surfactant	Background solution

Figure 1: Diagram of experimental set-up for column experiments

Flow characterization inside the columns was carried out by tracer transport experiments. Prior to tracer and surfactant transport experiments, around 10 porous volumes (PV) of background solution were injected to achieve a constant conductivity of the effluent at column outlet. For tracer experiments, one pore volume of a 10^{-2} mol.L^{-1} KBr was used as the tracer solution. It was injected at the top of the column, and it was directly followed by the 10^{-4} mol.L^{-1} NaCl background solution until conductivity reached the background levels. The outlet conductivity of tracer in the effluent was continuously measured by a conductivity probe and then converted to tracer concentration. Surfactant transport experiments were successively performed after each tracer experiment. A pulse of a one pore volume surfactant solution was injected at the top of the column and 1.5 mL of solution were collected every minute. Surfactant concentration for each sample collected was then estimated by colorimetric methods (Jain et al., 2020). All experiments were carried out in duplicates under steady state saturated flow conditions at two different Darcy velocities (0.37±0.1 and 0.72±0.1 cm.min^{-1}). The breakthrough curves (BTCs) of tracer/surfactant were plotted as the normalized effluent concentrations as a function of pore volumes. Mass balance of the tracer and surfactant were estimated by calculating the zero-order moment of the breakthrough curve (Bai et al., 2016).

2.3 Flow and surfactant transport modelling

A two region MIM (mobile-immobile) model, implemented in the Hydrus 1D software, was used to characterize water flow via solute tracer transport experiments. The later assumes that solute transport by convection is limited to the mobile water regions (θ_m/θ) and solutes are exchanged between the mobile and immobile (θ_{im}/θ) regions by diffusion, described with a first-order diffusive exchange process (α) between the two regions (Eq(1) and Eq(2)) (Šimůnek and Van Genuchten, 2008).

$$\theta_m \frac{\partial C_m}{\partial t} + \theta_{im} \frac{\partial C_{im}}{\partial t} = \theta_m D_m \frac{\partial^2 C_m}{\partial x^2} - q \frac{\partial C_m}{\partial x} \quad (1)$$

$$\theta_{im} \frac{\partial C_{im}}{\partial t} = \alpha (C_m - C_{im}) \quad (2)$$

where θ_m and θ_{im} are the volumetric water contents in both the mobile and immobile regions [-],θ is the total water content, C_m and C_{im} are the relative concentrations of mobile and immobile regions [kg.m^{-3}], D_m is the dispersion coefficient of mobile region [m^2.s^{-1}] and α is the solute exchange rate between the two regions [s^{-1}]. The ratio θ_m/θ was estimated to characterize the flow uniformity. High θ_m/θ values indicate uniform flow into the column (Bai et al., 2016). The dispersivity of the medium, λ [m], was estimated as: $\lambda = D_m * \theta_m / q$. For surfactant transport, a modified form of the advection-dispersion MIM equation with term for kinetic deposition site used for particles transport was considered as following (Šimůnek and Van Genuchten, 2008):

$$\theta \frac{\partial C}{\partial t} + \rho \frac{\partial s}{\partial t} = \frac{\partial}{\partial x}\left(\theta_m D \frac{\partial C}{\partial x}\right) - q \frac{\partial C}{\partial x} \quad (3)$$

where C is the solute concentration [kg.m^{-3}], t is the time [s], ρ is the sans bulk density [kg.m^{-3}], s is the surfactant concentration on solid phase [Nc.kg$^{-1}_{\text{porous media}}$], D is the dispersion coefficient [m^2.s^{-1}]. Similar to other works, it was assumed that surfactant exchange between the mobile and the immobile phase was limited, (α= 0) with surfactant exclusion from the immobile regions (C_{im} = S_{im} = 0). The equation for the mass transfer between liquid and solid phase was described by the Eq (4):

$$\rho \frac{\partial s}{\partial t} = \theta \Psi k_{att} C - k_d \rho s \quad (4)$$

where k_{att} and k_d are the solid-liquid interface first-order attachment and detachment coefficients, and ψ is the dimensionless retention function to account for time dependent deposition, described by a Langmuirian dynamic equation. Tracer transport parameters (θ_m, λ and α) and surfactant transport (θ_m, λ) and deposition (k_{att}, k_d and s_{max}) parameters, were obtained by fitting the model to experimental data, by using Hydrus inverse solution procedure.

3. Results and discussion

3.1 Batch experiments

Batch experiments showed that a pseudo-equilibrium was reached after 24 h. At the pseudo-equilibrium time, surfactant quantity retained on sand was 0.794×10^{-6} mol.m^{-2} of porous media. This quantity was lower than the surface excess, which is the maximum adsorption density. Therefore, it was not possible to know if there was a monolayer of surfactant or aggregate, because the solid surface was not totally recovered by the surfactant. It could be interesting to continue experiments with higher concentrations for soil remediation ([C] > CMC). However, it will probably lead to the saturation of the solid surface or to the formation of aggregates in the case of hydrophilic surface (Paria, 2008).

3.2 Tracer and surfactant in dynamic column experiments

Experimental and simulated tracer and surfactant breakthrough curves (BTC) obtained for all operational conditions are presented in Figure 2. Similar shapes of tracer BTCs were obtained for both flow rates, while surfactant BTCs exhibited a distinct behavior, depending both on flow rate and surfactant concentration. Mass balance calculations equaled to 100% for all tracer experiments and they ranged from 34 to 85% for surfactant experiments, indicating surfactant retention in the porous media.

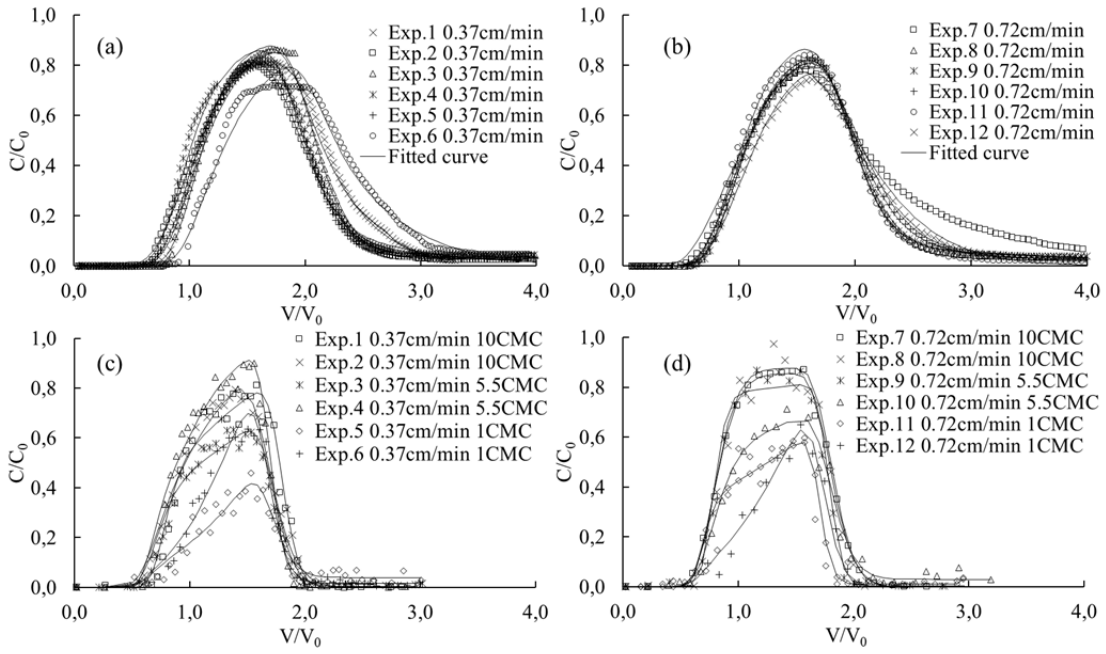

Figure 2: Measured (symbols) and fitted (lines) breakthrough curves of (a) tracer at low flow rate, (b) tracer at high flow rate, (c) surfactant at low flow rate and (d) surfactant at high flow through sandy porous media

Simulations of tracer elution curves showed similar dispersivity (λ), solute exchange rate (α) and mobile water contents for both flow rates. Thus, the mobile water regions ranged from 66 to 85% of the total water volume for all experiments. This means that 66 to 85 % of the pores represent flowing regions where solutes are transported by convection and dispersion process. The remaining pore volume (15 to 44%) is assumed to be immobile water region. This pore volume may represent immobile zones that can exchange and retain solutes by diffusion, but do not permit convective flow. Numerical simulation of surfactant transport showed that, similar to water tracer, they were mainly moved by convective flow (the mobile water regions ranged from 69 to 96%, Table 1), and no significant difference was obtained for both flowrate conditions. These results

indicated a useful information on surfactant transport uniformity. Indeed, a uniform transport could increase pollutant desorption and remediation efficiency.

Table 1: Surfactant transport and retention parameters obtained by MIM model

Replicate	$C_{initial}$ [CMC]	Effluent Recovery (%)	R^2 modified MIM model	λ [cm]	θ_{im}	θ_m/θ [%]	S_{max}	k_{att} [L.min^{-1}]	k_{det} [L.min^{-1}]
			Low flowrate						
Exp.1	10	64	0.98	0.15	0.01	96	0.19	0.05	$8.92\ 10^{-6}$
Exp.2	10	63	0.99	0.31	0.02	94	0.18	0.06	$1.56\ 10^{-4}$
Exp.3	5.5	74	0.98	0.26	0.12	74	0.33	0.07	$4.11\ 10^{-4}$
Exp.4	5.5	72	0.99	0.16	0.14	69	0.14	0.08	$6.23\ 10^{-3}$
Exp.5	1	34	0.93	0.30	0.11	73	0.94	0.17	$3.69\ 10^{-3}$
Exp.6	1	44	0.97	0.17	0.00	99	0.55	0.21	$1.74\ 10^{-3}$
			High flowrate						
Exp.7	10	84	1.00	0.27	0.08	82	0.58	0.02	$9.26\ 10^{-6}$
Exp.8	10	85	0.98	0.25	0.08	82	0.35	0.02	$8.71\ 10^{-6}$
Exp.9	5.5	79	0.99	0.10	0.10	79	0.36	0.03	$1.01\ 10^{-3}$
Exp.10	5.5	83	0.98	0.28	0.08	82	0.32	0.07	$8.78\ 10^{-3}$
Exp.11	1	67	0.90	0.10	0.14	70	0.50	0.14	$2.12\ 10^{-3}$
Exp.12	1	41	0.98	0.17	0.02	95	0.62	0.32	$1.77\ 10^{-6}$

Surfactant column experiments showed that the increasing of surfactant concentration will increase the relative surfactant recovery (Figure 3). However, similar surfactant recovery was obtained for experiment performed with 5.5 and 10 CMC. The 5.5 CMC concentration experiments permitted to obtain a concentration above the CMC at the column outlet, involving lower surfactant consumption in comparison to 10 CMC solution. Surfactant recovery slightly increased with increasing flow rate, probably due to lower surfactant residence time for experiments performed at high flow rate.

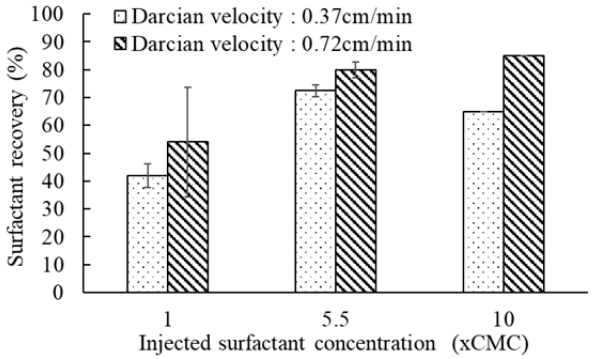

Figure 3: Surfactant recovery after column transport experiments

When surfactant concentration represents 1 CMC due to CSAC barrier (critical surface aggregation concentration), monomers may be present in solution, and this condition is not appropriated for soil remediation. Indeed, pollutant solubilization increases when the concentration exceeds the CMC. These results showed that Sisterna L70-C surfactant had an increasing affinity for the solid grains when the surfactant concentration decreases. However, surfactant irreversible retention onto the sand was obtained for all experiments. This was confirmed by attachment/detachment coefficients obtained from numerical simulations (Table 1). Indeed, attachment coefficients were much greater than detachment coefficients, indicating that surfactant retention was an irreversible process. Physico-chemical sand properties surface could be a plausible explanation of surfactant irreversible retention.

4. Conclusions

In this work, batch and column experiments using a nonionic sucrose ester surfactant, Sisterna L70-C, showed that this surfactant exhibited desirable characteristics for use in soil remediation, due to the low cost, appropriated transport properties and relatively low adsorption rates on porous media. The experiments performed under high flow rate combined with high surfactant concentration provided the best conditions for high surfactant recovery, which can be a practical implication to reduce surfactant retention during remediation process. Experimented performed with an intermediate concentration at 5.5 CMC, under high flow rate were more appropriated to obtain low surfactant retention (low consumption), while maintaining a necessary concentration (C>CMC in the effluent) for pollutant desorption. Surfactant transport and retention modelling provided an estimation of surfactant transport uniformity and irreversible surfactant retention. This information has a practical importance for the understating of the mechanisms of interactions, involved between surfactant and solid/water interfaces, and they should be considered for efficient pollutant desorption. This study should be completed by pollutant desorption experiments, by using the same experimental device with homogenous and heterogenous porous media, to confirm Sisterna L70-C potential use for soil remediation contaminated by hydrophobic compounds.

References

Almeida D. G., Soares da Silva R. C. F., Brasileiro P. P. F., Luna J. M., Silva M. G. C., Rufino R. D., Costa A. F. C., Santos V. A., Sarubbo L. A., 2018, Application of a Biosurfactant from Candida tropicalis UCP 0996 produced in low-cost substrates for hydrophobic contaminants removal, Chemical Engineering Transactions, 64, 541–546.

Almeida F. C. G., Rocha e Silva N. M., Souza T. C., Almeida D.G., Luna J. M., Farias C.B.B., Rufino R. D., Sarubbo L. A., 2019, Surfactant activity of artocarpus heterophyllu fruit extract and application in oil removal of solid surface, Chemical Engineering Transactions, 74, 1135–1140.

Bai H., Cochet N., Drelich A., Paus A., Lamy E., 2016, Comparison of transport between two bacteria in saturated porous media with distinct pore size distribution, RSC Advances, 6, 14602–14614.

Bhairi S. M, Mohan, C., Ibryamova S., and LaFavor T., 2017, Detergents: A guide to the properties and uses of detergents in biological systems < https://www.sigmaaldrich.com/content/dam/sigma-aldrich/1/content/commerce/pdfs/detergents/detergents-guide-mk.pdf>

Cecotti M., Coppotelli B.M., Mora V.C., Viera M., Morelli I.S., 2018, Efficiency of surfactant-enhanced bioremediation of aged polycyclic aromatic hydrocarbon-contaminated soil: Link with bioavailability and the dynamics of the bacterial community, Science of The Total Environment, 634, 224–234.

Gabet S., 2004, Remobilisation d'Hydrocarbures Aromatiques Polycycliques (HAP) présents dans les sols contaminés à l'aide d'un tensioactif d'origine biologique, PhD Thesis, Université de Limoges, France.

Jain A., Jain R., Jain S., 2020, Quantitative analysis of reducing sugars by 3, 5-Dinitrosalicylic acid (DNSA method). In Basic Techniques in Biochemistry, Microbiology and molecular Biology: principles and techniques, eds. (New York, NY: Springer US), pp. 181–183.

Lau E.V., Gan S., Ng H.K., Poh P.E., 2014, Extraction agents for the removal of polycyclic aromatic hydrocarbons (PAHs) from soil in soil washing technologies, Environmental Pollution, 184, 640–649.

Mao X., Jiang R., Xiao W., Yu J., 2015, Use of surfactants for the remediation of contaminated soils: a review, Journal of Hazardous Materials, 285, 419–435.

Mercado-Pacheco J., Julio-Altamiranda Y., Sánchez-Tuirán E., González-Delgado Á.D., Ojeda K.A., 2020, Variables affecting delignification of corn wastes using urea for total reducing sugars production, ACS Omega, 5, 12196–12201.

Mulligan C.N., 2017, Biosurfactants for the remediation, Chapter In: DAS S, Dash HR (Ed.) Handbook of Metal-Microbe Interactions and Bioremediation, CRC Press, p.p. 299-314.

Paria S., 2008, Surfactant-enhanced remediation of organic contaminated soil and water, Advances in Colloid and Interface Science, 138, 24–58.

Rosen M.J. and Kunjappu J.T. (Ed.) 2012, Surfactants and interfacial phenomena, 4th Edition, John Wiley & Sons Ltd., New York.

Salager J. L., Forgiarini A.M., Rondón M.J., 2017, How to attain ultralow interfacial tension and three-phase behavior with a surfactant formulation for enhanced oil recovery: a Review—Part 3. Practical procedures to optimize the laboratory research according to the current state of the art in surfactant mixing, Journal of Surfactants and Detergents, 20, 3–19.

Šimůnek J., and Van Genuchten M.T., 2008, Modeling nonequilibrium flow and transport processes using HYDRUS, Vadose Zone Journal, 7, 782–797.

Yin P., Zhou W., Pan R., Gao S., Mao X., 2016, Remediation of 2,4,6-Trichlorophenol contaminated soils by a combination use of surfactant-washing and bioaugmentation, Microbiological Research, 42, 104–110.